

Prediction of shrinkage Porosity Defect in Sand Casting Process of LM25

¹ H.P.Rathod,² N.P.Maniar,³ J.K.Dhulia
¹P.G.Student,²Assistant Professor,³Assistant Professor

ABSTRACT

In the present worldwide and aggressive environment foundry commercial enterprises needs to perform productively with least number of dismissals. Likewise they need to create throwing segments in short lead time. Foundry industry experiences low quality and profitability because of different procedure parameters. Interest of imperfection free throwing and strict conveyance calendar are required however the foundries are discovering it extremely hard to meet. Desert free castings with least generation cost have turned into the need of the foundries. The procedure of throwing cementing is intricate in nature and re-enactment of such process is required in industry before it is really attempted. The imperfections like shrinkage hole, porosity and sink can be minimized by planning and proper sustaining framework to guarantee directional cementing in the throwing, prompting feeders. This study is expected to survey the examination work made by a few analysts for expectation of the sum and size of the shrinkage porosity in sand throwing. The expectation of porosity is required in light of the fact that if porosity is distinguished as gas porosity and the pouring temperature is brought down to diminish the same, it might prompt different imperfections like cold shut.

IndexTerms - Sand casting, casting defects, defect analysis, Shrinkage porosity, aluminium alloy, casting simulation.

I. INTRODUCTION

Casting is the most established known procedure to deliver metallic parts. The primary metal casting was done by utilizing stone and metal moulds. After that various processes have been developed. In casting the molten metal is poured into mould relating to the desired shape (geometry). The shape obtain in the liquid material is now made by solidification and can be removed from the mould as a solid component.

Sand casting is one of the oldest method used for metal casting. It needs the shape of the desired casting called pattern in sand to make an imprint gating system, filling the cavity by molten metal, allowing it to solidify and then breaking away the sand mould and remove the desired component.

Casting process still have problems like quality maintaining, low production, low energy efficiency and more material consumption. In solidification process different type of defects are possible to occur which cannot be eliminated by making changes in process parameters, one such defect is shrinkage porosity.

These defects can be minimized by using methodology and simulation software. The engineer will decides the casting process, cores, parting line, moulds, gating system, etc. and analyses each parameter to how the design could be modify in such a way that it reduces defects.

II. Prediction of Shrinkage Porosity Using ANSYS and NDT

Casting Junctions:

A casting junction is an abrupt increase in local thickness caused by meeting of two or more elements (walls) resulting in regions of high thermal concentration. Molten metal at the junction cools slowly, leading to shrinkage porosity defects. The size and extent of defect region depends on the thickness and number of elements, and the angle between them, all of which affect the rate of heat transfer from the casting.

Classification of Casting Junction

A general characterization of junctions with N number of elements (or walls) is proposed here, based on section attributes, section orientation, additional geometric features, and feedability properties. These are described here.

(a) Section attributes (for each element)

- L - Length of element
- t - Thickness of element
- h - Height
- r - Fillet radius

(b) Section orientation (for each element)

- θ , Φ - Angular references

(c) Additional geometric features

- A - Cross-section area
- h/t - Extent of contact between adjacent element:
- Cross-section type: (R) rectangular, (C) circular, (O) oval, (FF) freeform
- Central hole (if present): shape, surface area

- Plane orthogonal to junction: Number of such planes and their section properties, offset of such planes from junction and their orientation.

Figure 1 Junction parameters and types

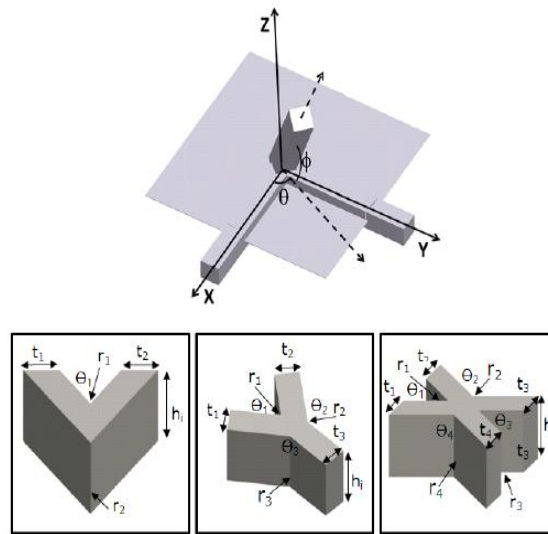
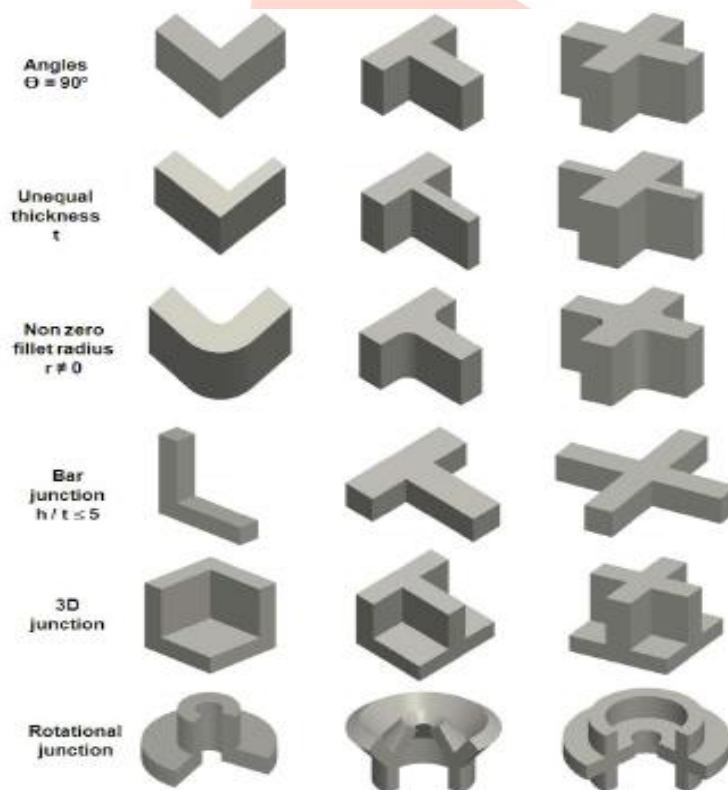


Figure 2 Junction Classification



III. EXPERIMENTS ON LM25

Moulding Sand:

Silica sand moulds are prepared using sand mix with a composition of 8% calcium based bentonite, 4% moisture (approx.) and 2% saw dust and coal powder are added.

Melting and Pouring:

The LM25 Aluminum alloys are melted in and As soon as the molten metal reaches a temperature of 750°C, it is taken out. The presence of oxides and coal ash in the surface of the molten metal are skimmed. Then the molten metal is poured into the mould cavity at a temperature of 750°C.

Table 1 Nomenclatures

Nomenclature	Arm length	Angle	Width
Y-30-40-10	30	40	10
Y-30-50-15	30	50	15
Y-30-60-20	30	60	20
Y-45-40-15	45	40	15
Y-45-50-20	45	50	20
Y-45-60-10	45	60	10
Y-60-40-20	60	40	20
Y-60-50-10	60	50	10
Y-60-60-15	60	60	15

Figure 3 Wood Pattern



Figure 4 Moulding box (Vijay Foundry)



Figure 5 Pouring of Casting (Vijay Foundry)



Table 2 Experimental Setup

Size of moulding box	330 mm ×330 mm
Pouring Temperature	700°C,725°C,750°C
Feeder	Not used
No. of Cavity	9

Table 3 Chemical Composition of LM 25

Sr. No.	Element	Weight (%)
1	Copper	0.1 max
2	Magnesium	0.20-0.60
3	Silicon	6.5-7.5
4	Iron	0.5 max
5	Manganese	0.3 max
6	Nickel	0.1 max
7	Zinc	0.1 max
8	Lead	0.1 max
9	Tin	0.05 max
10	Titanium	0.2 max
11	Alluminium	Remainder

➤ Analysis of Cast Parts using Ansys 15.0

Table 4 Input Parameters For Simulation

Load condition	
Ref. Temp	300 K
Initial condition of Metal (Pouring temperature)	973/998/1023 k
Initial condition of sand	300 k
Load step	1
Time	1000
Time step size	1

Figure 6 Steady State Thermal Solution For Part 1

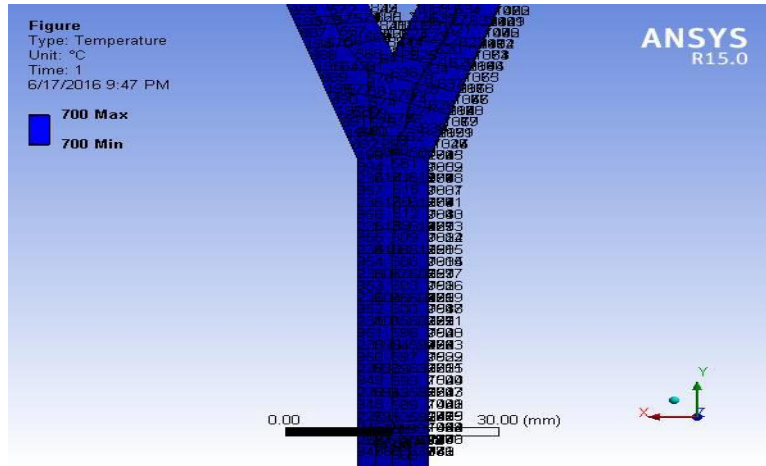


Figure 7 Transient Thermal Solution For Part 1

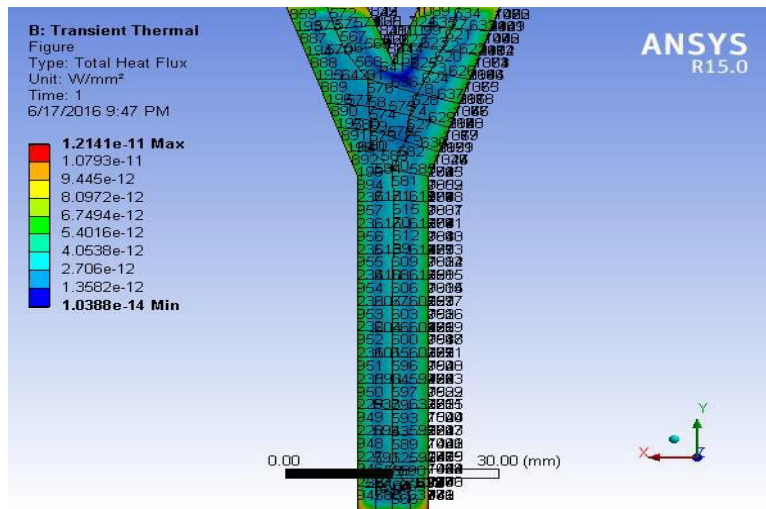


Figure 8 Steady State Thermal Solution For Part 2

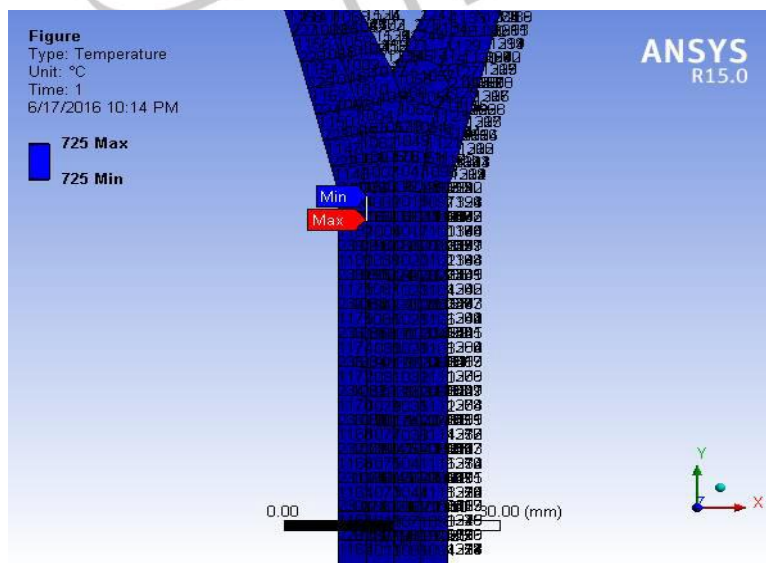


Figure 9 Transient Thermal Solution For Part 2

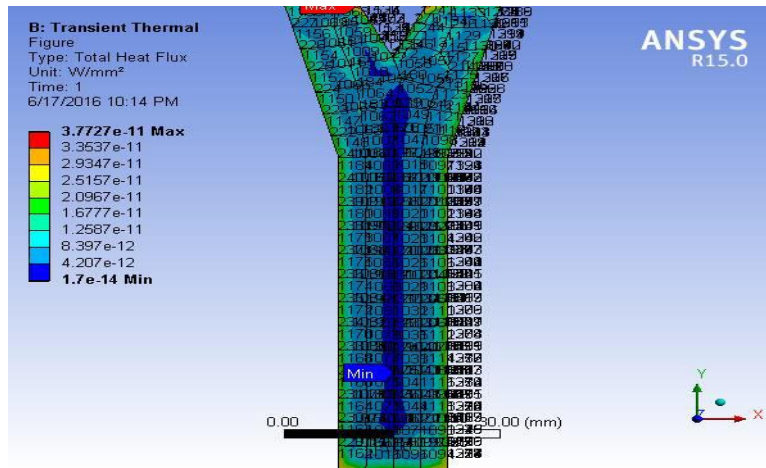


Figure 10 Steady State Thermal Solution For Part 3

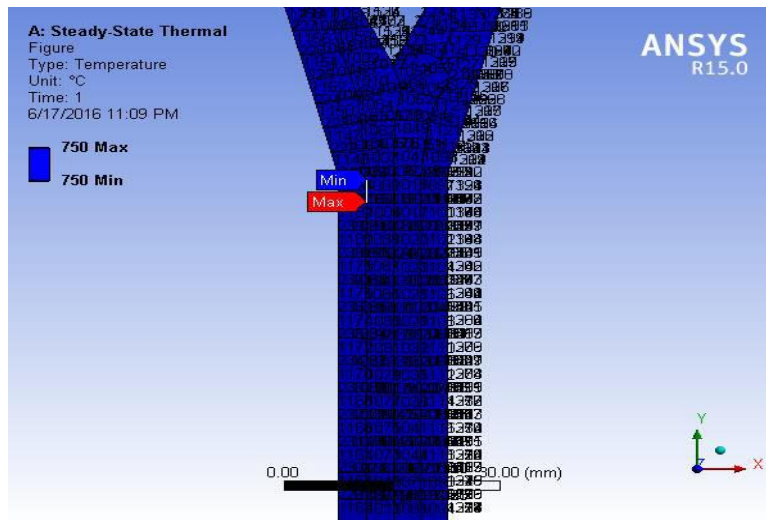


Figure 11 Transient Thermal Solution For Part 3

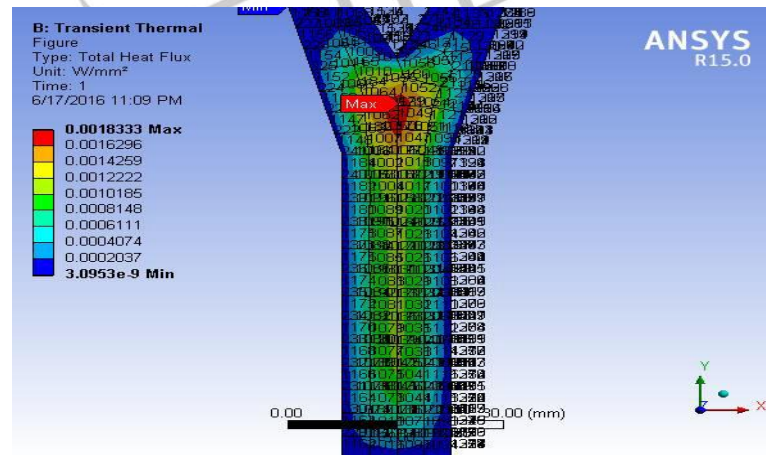


Figure 12 Steady State Thermal Solution For Part 4

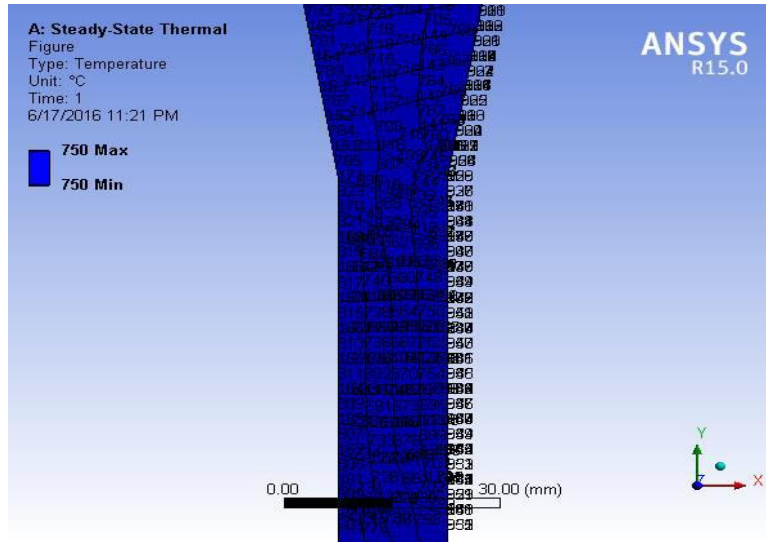


Figure 13 Transient Thermal Solution For Part 4

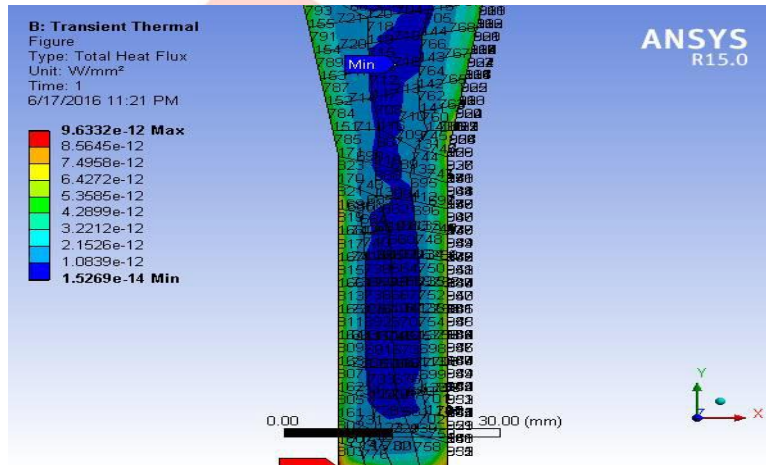


Figure 14 Steady State Thermal Solution For Part 5

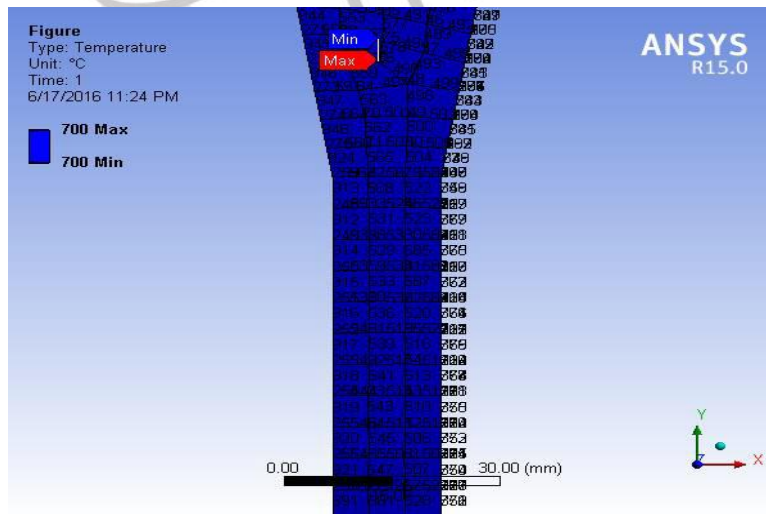


Figure 15 Transient Thermal Solution For Part 5

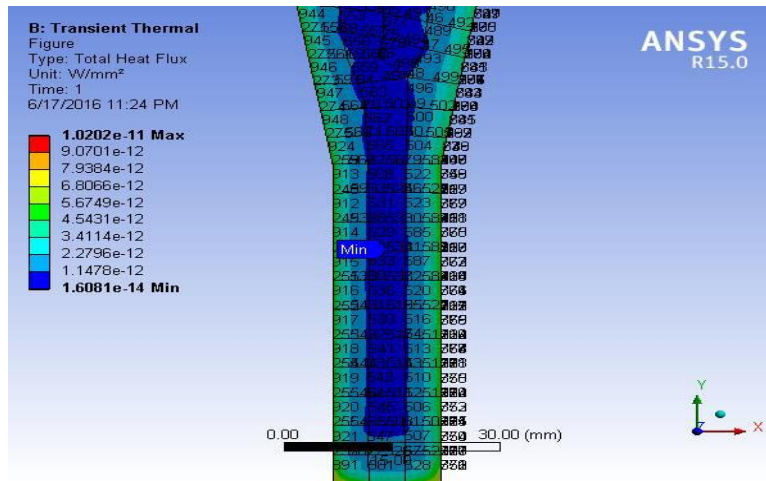


Figure 16 Steady State Thermal Solution For Part 6

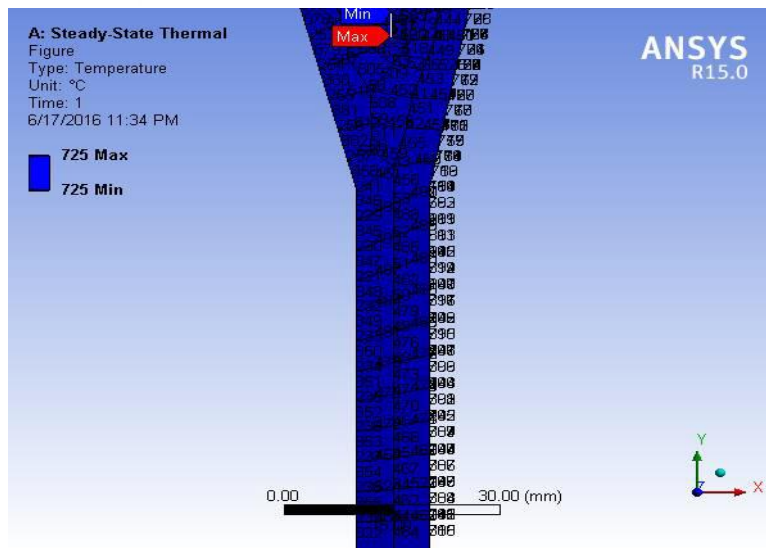


Figure 17 Transient Thermal Solution For Part 6

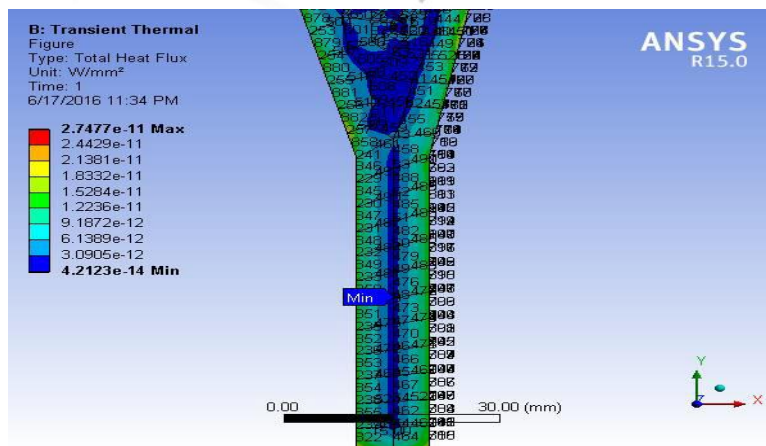


Figure 18 Steady State Thermal Solution For Part 7

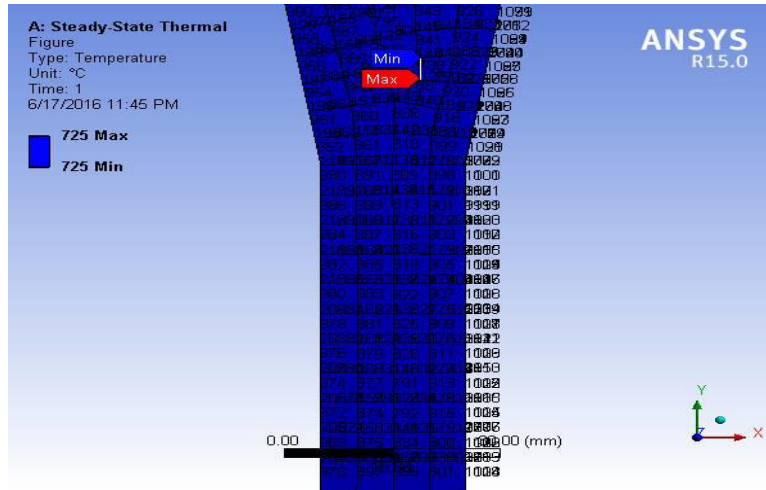


Figure 19 Transient Thermal Solution For Part 7

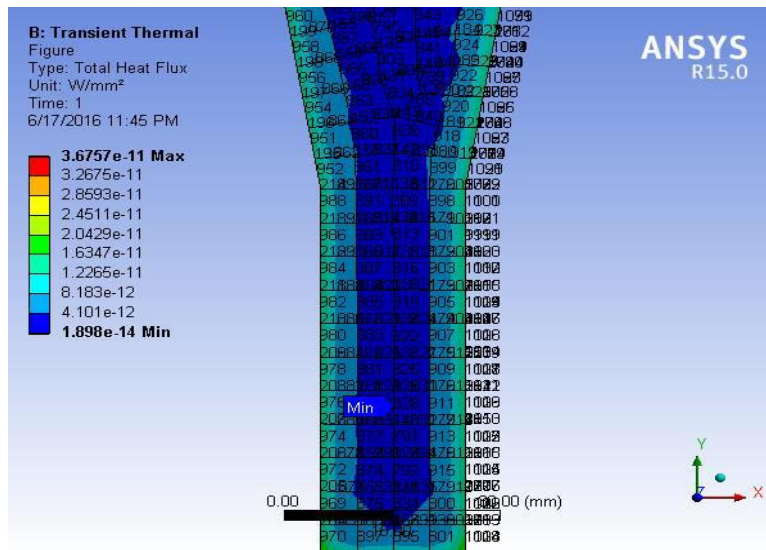


Figure 20 Steady State Thermal Solution For Part 8

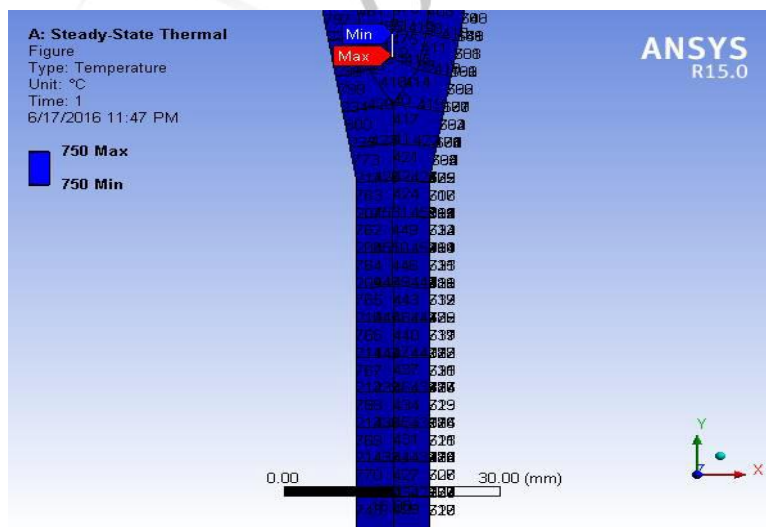


Figure 21 Transient Thermal Solution For Part 8

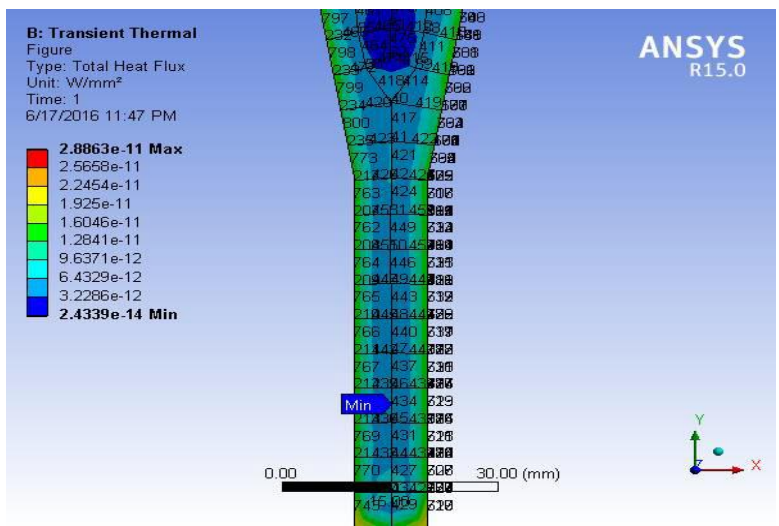


Figure 22 Steady State Thermal Solution For Part 9

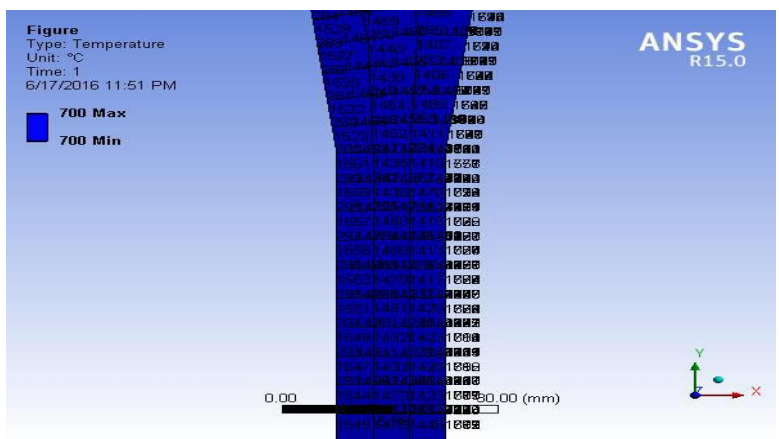
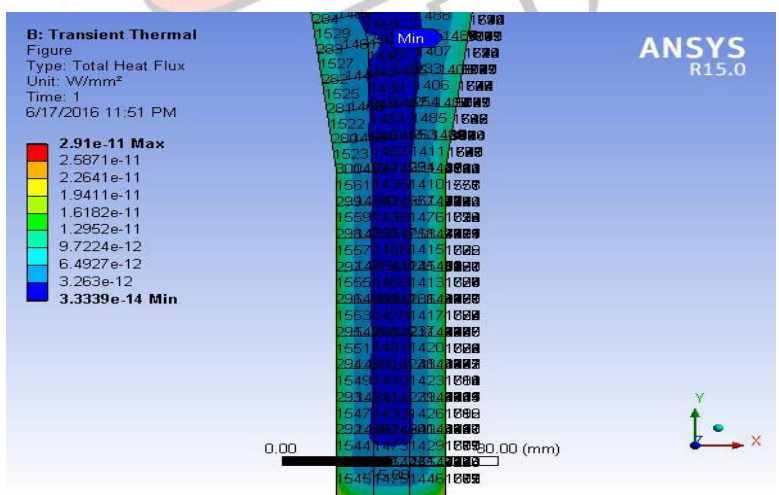


Figure 23 Transient Thermal Solution For Part 9



➤ **Non Destructive Testing of Cast Parts**

Nondestructive testing (NDT) is the process of inspecting, testing, or evaluating materials, components or assemblies for discontinuities, or differences in characteristics without destroying the serviceability of the part or system. In other words, when the inspection or test is completed the part can still be used.

In contrast to NDT, other tests are destructive in nature and are therefore done on a limited number of samples ("lot sampling"), rather than on the materials, components or assemblies actually being put into service.

These destructive tests are often used to determine the physical properties of materials such as impact resistance, ductility, yield and ultimate tensile strength, fracture toughness and fatigue strength, but discontinuities and differences in material characteristics are more effectively found by NDT.

Today modern nondestructive tests are used in manufacturing, fabrication and in-service inspections to ensure product integrity and reliability, to control manufacturing processes, lower production costs and to maintain a uniform quality level. During construction, NDT is used to ensure the quality of materials and joining processes during the fabrication and erection phases, and in-service NDT inspections are used to ensure that the products in use continue to have the integrity necessary to ensure their usefulness and the safety of the public.

It should be noted that while the medical field uses many of the same processes, the term "nondestructive testing" is generally not used to describe medical applications.

➤ **NDT Test Methods**

Test method names often refer to the type of penetrating medium or the equipment used to perform that test. Current NDT methods are: Acoustic Emission Testing (AE), Electromagnetic Testing (ET), Guided Wave Testing (GW), Ground Penetrating Radar (GPR), Laser Testing Methods (LM), Leak Testing (LT), Magnetic Flux Leakage (MFL), Microwave Testing, Liquid Penetrant Testing (PT), Magnetic Particle Testing (MT), Neutron Radiographic Testing (NR), Radiographic Testing (RT), Thermal/Infrared Testing (IR), Ultrasonic Testing (UT), Vibration Analysis (VA) and Visual Testing (VT).

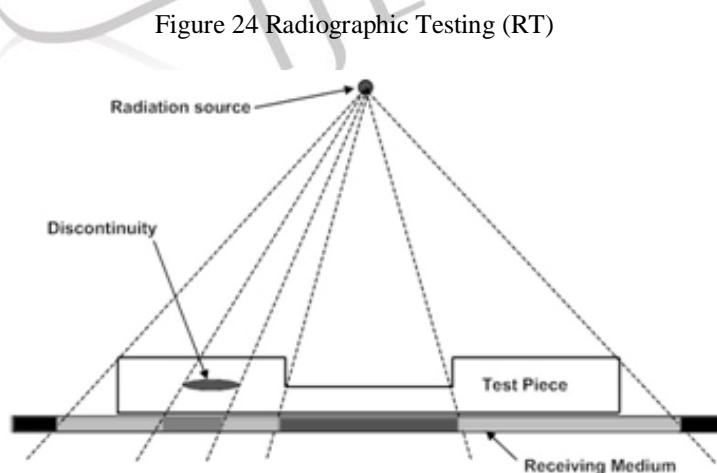
➤ **Radiographic Testing (RT)**

X-rays are used to produce images of objects using film or other detector that is sensitive to radiation. The test object is placed between the radiation source and detector. The thickness and the density of the material that X-rays must penetrate affects the amount of radiation reaching the detector. This variation in radiation produces an image on the detector that often shows internal features of the test object.

Industrial radiography involves exposing a test object to penetrating radiation so that the radiation passes through the object being inspected and a recording medium placed against the opposite side of that object. For thinner or less dense materials such as aluminum, electrically generated x-radiation (X-rays) are commonly used, and for thicker or denser materials, gamma radiation is generally used.

Gamma radiation is given off by decaying radioactive materials, with the two most commonly used sources of gamma radiation being Iridium-192 (Ir-192) and Cobalt-60 (Co-60). IR-192 is generally used for steel up to 2-1/2 - 3 inches, depending on the Curie strength of the source, and Co-60 is usually used for thicker materials due to its greater penetrating ability.

The recording media can be industrial x-ray film or one of several types of digital radiation detectors. With both, the radiation passing through the test object exposes the media, causing an end effect of having darker areas where more radiation has passed through the part and lighter areas where less radiation has penetrated. If there is a void or defect in the part, more radiation passes through, causing a darker image on the film or detector, as shown in Figure



➤ X-Ray Film of Cast Parts

Figure 25 X-Ray Film For Part 1



Figure 26 X-Ray Film For Part 2



Figure 27 X-Ray Film For Part 3

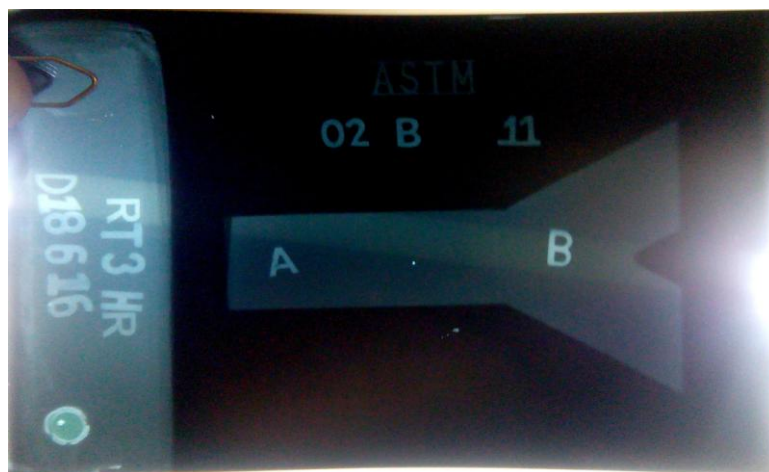


Figure 28 X-Ray Film For Part 4



Figure 29 X-Ray Film For Part 5



Figure 30 X-Ray Film For Part 6

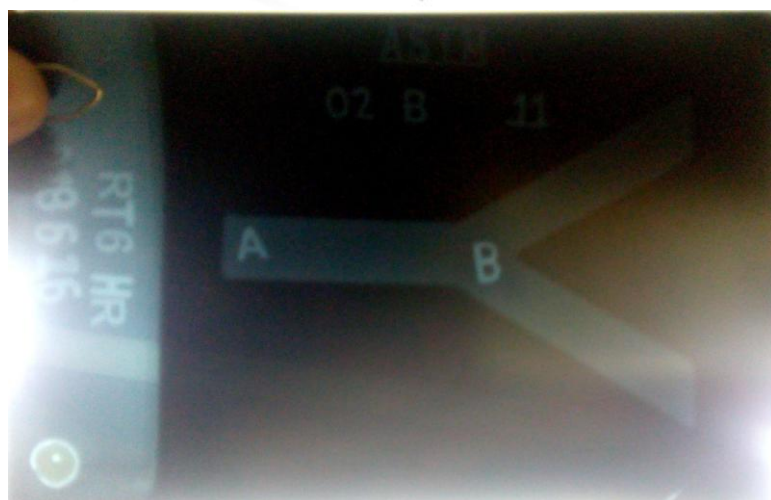


Figure 31 X-Ray Film For Part 7

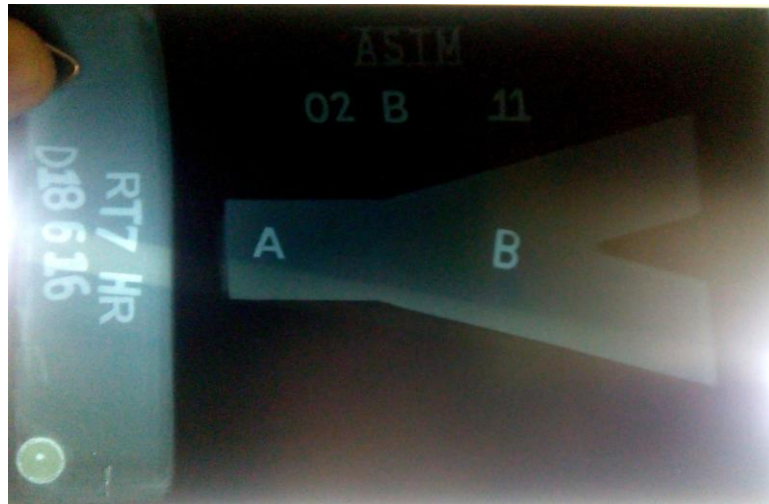


Figure 32 X-Ray Film For Part 8

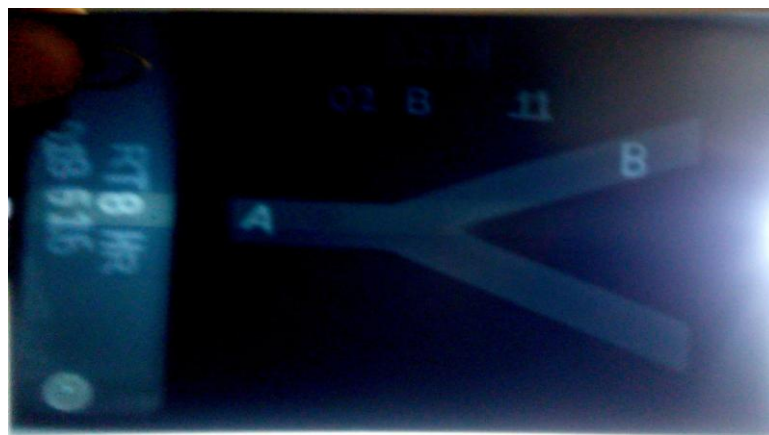


Figure 33 X-Ray Film For Part 9



IV. EMPIRICAL MODEL DEVELOPMENT

Following approach is used to develop bridge between experimental data and simulation software ANSYS.

Arm length (L), Arm thickness (t) and Arm angle (θ) have been taken as geometric parameters for development of empirical model.

Arm length (L) = 30, 45, 60

Arm angle (θ) = 40, 50, 60

Arm thickness (t) = 10, 15, 20

Thermal gradient (G) and Cooling rate (r) have been taken as thermal parameter for development of empirical model. Observations were made of location of shrinkage porosity for each Y- junction casting.

Regression analysis

Regression analysis is used to investigate and model the relationship between a response variable and one or more predictors. It is well defined function. It is based upon least squares method and calculates equation of straight line (in the form of equation 5.1) that best fits data.

$$y = m_1x_1 + m_2x_2 + m_3x_3 + m_4x_4 + \dots + m_nx_n + b \dots \text{eqn. (1.1)}$$

Where, the dependent y-value is a function of the independent x-values. The m-values are coefficient corresponding to each x-value and b is a constant value.

Regression can be carried out using either Minitab® or Microsoft Excel®. The interpretation of results is also very important task. The results of regression analysis are interpreted in following manner.

- R Square is measure of the explanatory power of the model. In theory, R square compares the amount of the error explained by the model as compared to the amount of error explained by averages. The higher the R-Square better the result. An R-Square above .5 is generally considered quite well.
- Adjusted R Square is a modified version of R Square, and has the same meaning, but includes computations that prevent a high volume of data points from artificially driving up the measure of explanatory power. An Adjust R Square above .20 is generally considered quite well.
- The t-statistic is a measure of how strongly a particular independent variable explains variations in the dependent variable. The larger the t-statistic is the good for model.
- The P-value is the probability that the independent variable in question has nothing to do with the dependent variable. It should be less than 0.1.
- F is similar to the t-stat, but F looks at the quality of the entire model, meaning with all independent variables included. The larger the F is better.
- Regression analysis is carried out to develop the empirical model which will provide quantitative prediction of shrinkage porosity using Minitab. The regression statistics are as given in table. Results from regression analysis are shown in table.

Table 5 Experimental and Simulation Data

ln(r)	ln(G)	ln(L)	ln(t)	ln(θ)	ln(N_y^*)
0.077801	-0.57005	1.47712	1	1.60205	-0.60896
0.077636	-0.99675	1.47712	1	1.60205	-1.03558
0.077636	-1.04815	1.47712	1	1.60205	-1.08697
0.077677	-0.72916	1.47712	1	1.60205	-0.768
0.077822	-0.5528	1.47712	1	1.60205	-0.59171
0.077801	-0.53255	1.47712	1	1.60205	-0.57146
0.077698	-0.68596	1.47712	1	1.60205	-0.72481
-0.086747	-0.77851	1.47712	1.17609	1.69897	-0.73513
-0.086747	-0.809	1.47712	1.17609	1.69897	-0.76562
-0.086664	-0.62258	1.47712	1.17609	1.69897	-0.57925
-0.086789	-0.95347	1.47712	1.17609	1.69897	-0.91007
-0.086789	-1.07212	1.65321	1.17609	1.69897	-0.91007
-0.086706	-0.6881	1.65321	1.17609	1.69897	-1.02873
-0.086706	-0.65942	1.65321	1.17609	1.69897	-0.64475
0.271842	-0.54804	1.65321	1.17609	1.60205	-0.61606
0.271677	-1.30552	1.65321	1.17609	1.60205	-0.61606
0.271748	-0.73166	1.65321	1.17609	1.60205	-0.68396
0.271771	-0.53925	1.65321	1.17609	1.60205	-1.44135
0.271795	-0.49838	1.65321	1.17609	1.60205	-0.59171
-0.393812	2.92179	1.65321	1	1.60205	-0.86753
-0.473183	2.92181	1.65321	1	1.60205	-0.86753
-0.578495	2.92181	1.77815	1	1.60205	-0.63428
-0.578495	2.92179	1.77815	1	1.60205	-0.54827
-0.086789	2.92179	1.77815	1	1.60205	-0.54827
-0.086789	0.49838	1.65321	1.30102	1.77815	-0.64475
0.077698	2.92181	1.65321	1.30102	1.77815	-0.62759
-0.086747	2.92181	1.65321	1.30102	1.77815	-0.73291

Following points should be observed from regression analysis.

- R Square is **0.974** which is acceptable and Adjusted R square **0.966** which is acceptable.
- The P – value of each variable are acceptable.
- Thermal Gradient having highest t-stat value and lowest P- value. It means Gradient highly affects on porosity formation.
- Regression model can be given as

$$\ln(N_y^*) = -0.245 - 0.500 \ln(r) + 1.00 \ln(G) + 0.17 \ln(L) + 0.124 \ln(t) - 0.268 \ln(\theta) \dots \dots \dots \text{(eq.1.2)}$$

So, equation can be written as

$$N_y^* = \frac{\ln(G)\ln(L)^{0.17}\ln(t)^{0.124}}{(0.897)\ln(r)^{0.5}\ln(\theta)^{0.268}} \dots \dots \dots \text{(eq.1.3)}$$

Table 6 Regression Statistics

R Square	97.4 %
Adjusted R Square	96.6 %
Standard Error	0.154
Observations	27

Table 7 Regression Analysis

	Coefficients	t Stat	P-value
Intercept	0.245	-1.29	0.115
ln(G)	1.0000	1586282.98	0.000
ln(r)	-0.500001	-359728.30	0.000
ln(L)	0.17	1.65	0.103
ln(t)	0.124	0.72	0.473
ln(θ)	-0.268	-0.93	0.356

V. Conclusion and Results

From experimental results it is clear that for Y junction there is more chances of shrinkage porosity occurrence near the center of geometry. The location of shrinkage porosity can vary according to geometric and thermal parameter change. From experimental results, it can be observed that large amount of shrinkage porosity were formed near the center as found in simulation. Experiments for Zink alloy considering geometric and thermal parameters.

REFERENCES

- [1] Kent D. Carlson, Zhiping Lin, Richard A. Hardin and Christoph Beckermann, “MODELING OF POROSITY FORMATION AND FEEDING FLOW IN STEEL CASTING” 2002.
- [2] S. Sulaiman, A.M.S. Hamouda “Modelling and experimental investigation of solidification process in sand casting” ELSEVIER Journal of Materials Processing Technology 155–156 (2004) 1723–1726.
- [3] A. Meneghini, L. Tomesani “Chill material and size effects on HTC evolution in sand casting of aluminum alloys” ELSEVIER Journal of Materials Processing Technology 162–163 (2005) 534–539.
- [4] Kent D. Carlson, Zhiping Lin, Christoph Beckermann, George Mazurkevich, and Marc C. Schneider “MODELING OF POROSITY FORMATION IN ALUMINUM ALLOYS” TMS (The Minerals, Metals & Materials Society), 2006.
- [5] Neelesh Jain, Kent D. Carlson and Christoph Beckermann “Round Robin Study to Assess Variations in Casting Simulation Niyama Criterion Predictions” 2007.
- [6] Kent D. Carlson and Christoph Beckermann “Use of the Niyama Criterion To Predict Shrinkage-Related Leaks in High-Nickel Steel and Nickel-Based Alloy Castings” 2008.
- [7] V.V.Mane, Amit Sata and M. Y. Khire “New Approach to Casting Defects Classification and Analysis Supported by Simulation” 2010.
- [8] M. V. Okseniuk, S. F. Gueijman, C. E. Schvezov, A. E. Ares “The influence of gravity on the CET in diluted Zn-Al alloys” ELSEVIER Procedia Materials Science 1 (2012) 64 – 71.

- [9] Nicoletto, Radomila Konecna, Stanislava Fintova “Characterization of microshrinkage casting defects of Al–Si alloys by X-ray computed tomography and metallography” *ELSEVIER International Journal of Fatigue* 41 (2012) 39–46.
- [10] Uday A. Dabade and Rahul C. Bhedasgaonkar “Casting Defect Analysis using Design of Experiments (DoE) and Computer Aided Casting Simulation Technique” *ELSEVIER Procedia CIRP* 7 (2013) 616 – 621.
- [11] Niels Skat Tiedje, John A. Taylor, Mark A. Easton “A new multi-zone model for porosity distribution in Al–Si alloy castings” *ELSEVIER Acta Materialia* 61 (2013) 3037–3049.
- [12] Hossein Bayani, Seyed Mohammad Hossein Mirbagheri, Mojtaba Barzegari, Sadegh Firoozi “Simulation of unconstrained solidification of A356 aluminum alloy on distribution of micro/macro shrinkage” *ELSEVIER j mater res technol.* 2014; 3(1):55–70.

